J. Chem. Thermodynamics 85 (2015) 68–76

Contents lists available at ScienceDirect

J. Chem. Thermodynamics

journal homepage: www.elsevier.com/locate/jct

Extended corresponding states expressions for the changes in enthalpy, compressibility factor and constant-volume heat capacity at vaporization

S. Velasco [a,b], M.J. Santos [a], J.A. White [a,b,*]

[a] Departamento de Física Aplicada, Universidad de Salamanca, 37008 Salamanca, Spain
[b] IUFFyM, Universidad de Salamanca, 37008 Salamanca, Spain

ARTICLE INFO

Article history:
Received 2 October 2014
Received in revised form 19 December 2014
Accepted 16 January 2015
Available online 31 January 2015

Keywords:
Vapor pressure curve
Saturation properties
Acentric factor
Enthalpy of vaporization
Compressibility factor
Constant-volume heat capacity

ABSTRACT

By analyzing data for the vapor pressure curve of 121 fluids considered by the National Institute of Standards and Technology (NIST) program RefProp 9.1, we find that the first and the second derivatives with respect to reduced temperature (T_r) of the natural logarithm of the reduced vapor pressure at the acentric point ($T_r = 0.7$) show a well defined behavior with the acentric factor ω. This fact is used for checking some well-known vapor pressure equations in the extended Pitzer corresponding states scheme. In this scheme, we then obtain analytical expressions for the temperature dependence of the enthalpy of vaporization and the changes in the compressibility factor and the constant-volume heat capacity along the liquid–vapor coexistence curve. Comparisons with RefProp 9.1 results are presented for argon, propane and water. Furthermore, very good agreement is obtained when comparing with experimental data of perfluorobenzene and perfluoro-n-heptane.

1. Introduction

The vapor pressure equation for a pure fluid gives the relation between saturation pressure p_σ and temperature T from the triple to the critical point along the liquid–vapor phase boundary σ. The form of this equation is one of the most fascinating unsolved problems in physics. Perhaps, it is the equation for which a larger number of proposals have been made. The only two informations that thermodynamics provides about it concern to its first temperature derivative, the so-called Clapeyron–Clausius equation,

$$p'_\sigma(T) \equiv \frac{dp_\sigma}{dT} = \frac{\Delta_v \overline{H}}{T\left(\overline{V}^g - \overline{V}^l\right)}, \tag{1}$$

and to its second temperature derivative, the so-called Yang–Yang equation [1],

$$p''_\sigma(T) \equiv \frac{d^2 p_\sigma}{dT^2} = \frac{\overline{C}^g_{v2} - \overline{C}^l_{v2}}{T\left(\overline{V}^g - \overline{V}^l\right)}, \tag{2}$$

where $\Delta_v \overline{H}$ is the molar enthalpy of vaporization, $\overline{V}^g$ and $\overline{V}^l$ are the vapor (g) and liquid (l) molar volumes at saturation, and $\overline{C}^g_{v2}$ and $\overline{C}^l_{v2}$ are the two-phase vapor and liquid molar heat capacities at constant volume.

Equations (1) and (2) are exact thermodynamic relations, and they can be rewritten in different convenient forms that involve the natural logarithm of the vapor pressure as a function of the temperature. One of these forms for equation (1) is

$$\frac{d\ln p_\sigma}{dT} = \frac{\Delta_v \overline{H}}{RT^2 \Delta_v Z}, \tag{3}$$

where Z is the compressibility factor defined as $p_\sigma \overline{V}/RT$, R being the gas constant, and therefore $\Delta_v Z = Z^g - Z^l$ is the change in the compressibility factor associated to vaporization. On the other hand, taking into account the relationship

$$\frac{d^2 \ln p_\sigma}{dT^2} = -\left(\frac{d\ln p_\sigma}{dT}\right)^2 + \frac{1}{p_\sigma}\frac{d^2 p_\sigma}{dT^2}, \tag{4}$$

and using equations (2) and (3) one obtains

$$\frac{d^2 \ln p_\sigma}{dT^2} = -\left(\frac{\Delta_v \overline{H}}{RT^2 \Delta_v Z}\right)^2 + \frac{\Delta_v \overline{C}_v}{RT^2 \Delta_v Z}, \tag{5}$$

where $\Delta_v \overline{C}_v = \overline{C}^g_{v2} - \overline{C}^l_{v2}$. In terms of the reduced variables $T_r \equiv T/T_c$ and $p_r \equiv p_\sigma/p_c$, with T_c and p_c being the temperature and the pressure of the critical point, equation (3) becomes

* Corresponding author at: Departamento de Física Aplicada, Universidad de Salamanca, 37008 Salamanca, Spain. Tel.: +34 923294436; fax: +34 923294584.
E-mail address: white@usal.es (J.A. White).

http://dx.doi.org/10.1016/j.jct.2015.01.011
0021-9614/

$$\frac{d\ln p_r}{dT_r} = \frac{\Delta_v \overline{H}_r}{T_r^2 \Delta_v Z}, \tag{6}$$

where $\Delta_v \overline{H}_r = \Delta_v \overline{H}/RT_c$ is the reduced enthalpy of vaporization, while equation (5) becomes

$$\frac{d^2\ln p_r}{dT_r^2} = -\frac{1}{T_r^4}\left(\frac{\Delta_v \overline{H}_r}{\Delta_v Z}\right)^2 + \frac{1}{T_r^2}\frac{\Delta_v \overline{C}^*_v}{\Delta_v Z}, \tag{7}$$

where $\Delta_v \overline{C}^*_v = \left(\overline{C}^g_{v2} - \overline{C}^l_{v2}\right)/R$. If one knows the temperature dependence of the right-hand side of equations (6) or (7), integrations of these equations yield the vapor pressure curve. For example, by assuming a constant ratio $\Delta_v \overline{H}_r/\Delta_v Z$ and imposing that $p_r = 1$ at $T_r = 1$, integration of equation (6) leads to the so-called Clausius–Clapeyron (CC) equation,

$$\ln p_r = A\left(1 - \frac{1}{T_r}\right), \tag{8}$$

where the parameter A can be obtained from a known point in the vapor-pressure curve.

The two-parameter corresponding-states principle (CSP) states that fluids at equal reduced pressure and temperature should behave identically [2]. If the CSP were true, the parameter A in equation (8) should take the same value for all fluids. Guggenheim [3] proposed a value of $A \approx 5.4$ by fitting experimental vapor pressure data for a small number (seven) of nonpolar fluids. In order to extend the CSP to a wider range of fluids more parameters must be introduced in the corresponding-states correlations. In particular, in order to quantify the deviation of fluids with respect the two-parameter CSP predictions, Pitzer proposed in 1955 a third parameter ω, named *acentric factor* and defined as [4,5]

$$\omega \equiv -1.0 - \log_{10} p_r \quad \text{at} \quad T_r = 0.7, \tag{9}$$

Although the acentric factor was originally introduced to represent the nonsphericity (acentricity) of a molecule, nowadays it is used as a measure of the complexity of a molecule with respect to its size/shape and polarity and it is tabulated for many fluids [6]. Fluids with nearly $\omega = 0$ are called *simple* fluids (e.g., the seven Guggenheim's fluids). The Pitzer three-parameter CSP states that fluids with the same value of ω should behave identically at equal reduced pressure and temperature. We note that the acentric factor can be used to introduce the so-called acentric point given by $T = 0.7T_c$ and $p_\sigma = 10^{-(1+\omega)}p_c$.

In the Pitzer CSP theory, a vapor-pressure equation has the form

$$\ln p_r = f(T_r;\omega), \tag{10}$$

with $f(1;\omega) = 0$. Furthermore, taking into account definition (9), the function $f(T_r;\omega)$ must satisfy the condition

$$f(0.7;\omega) = -(1+\omega)\ln 10, \tag{11}$$

in order to be self-consistent at the acentric point. Recently [7] we have checked condition (11) for testing some vapor-pressure equations often used for estimating the vapor pressure of a large variety of fluids. In this work, we analyze the behavior of the first and second derivatives with respect the reduced temperature of $\ln p_r$ at the acentric point, i.e., the functions

$$f'(0.7;\omega) \equiv \left(\frac{d\ln p_r}{dT_r}\right)_{T_r=0.7} \tag{12}$$

and

$$f''(0.7;\omega) \equiv \left(\frac{d^2\ln p_r}{dT_r^2}\right)_{T_r=0.7}. \tag{13}$$

In particular, by using vapor-pressure data for the 121 fluids reported by the NIST program RefProp 9.1 [8], we find that both $f'(0.7;\omega)$ and $f''(0.7;\omega)$ show a well defined behavior with the acentric factor ω. This information can be used for testing vapor pressure equations or for obtaining adjustable coefficients appearing in them. On the other hand, in this work we also analyze the behavior of the reduced enthalpy of vaporization

$$\Delta_v \overline{H}_{r\omega} \equiv \Delta_v \overline{H}_r(T_r = 0.7), \tag{14}$$

the change in the compressibility factor

$$\Delta_v Z_\omega \equiv \Delta_v Z(T_r = 0.7), \tag{15}$$

and the change in the heat capacity at constant volume

$$\Delta_v \overline{C}^*_{v\omega} \equiv \Delta_v \overline{C}^*_v(T_r = 0.7), \tag{16}$$

at the acentric point. We find that $\Delta_v \overline{H}_{r\omega}$ is almost linearly correlated with ω while the ω-dependence of $\Delta_v Z_\omega$ and $\Delta_v \overline{C}^*_{v\omega}$ is well explained from $\Delta_v \overline{H}_{r\omega}, f'(0.7;\omega)$ and $f''(0.7;\omega)$. Finally, the obtained equations are used for predicting the effect of temperature on the reduced enthalpy of vaporization and on the changes in the compressibility factor and the constant-volume heat capacity during vaporization. We compare the obtained equations with NIST data for argon, propane and water and also with experimental data of perfluorobenzene and perfluoro-n-heptane, with very good agreement.

2. Checking vapor-pressure equations at the acentric point

The first temperature derivative of the natural logarithm of the vapor pressure at the acentric point, equation (12), can be obtained from equation (6),

$$f'(0.7;\omega) = \frac{\Delta_v \overline{H}_{r\omega}}{0.7^2 \Delta_v Z_\omega}, \tag{17}$$

with $\Delta_v \overline{H}_{r\omega}$ and $\Delta_v Z_\omega$ defined by equations (14) and (15), respectively. Figure 1(a) shows a plot of $f'(0.7;\omega)$ vs. ω. Symbols correspond to data obtained from RefProp 9.1 and equation (17) for the 121 substances listed in table 1. One can see that $f'(0.7;\omega)$ increases with ω in a practically linear way.

At this point it is important to remark that RefProp 9.1 is a computer program that uses the most accurate equations of state and models available for calculating a large number of properties for the 121 pure fluids included in the program [8]. Therefore, the results obtained from RefProp are not experimental data and, in some particular cases, are subjected to deviations that can be ascribed to the equation of state considered for the fluid. Nonetheless, in most cases RefProp 9.1 gives very accurate results that can be used to test the extended corresponding states expressions derived in this work.

The second temperature derivative of the natural logarithm of the vapor pressure at the acentric point, equation (13), can be obtained from equation (7)

$$f''(0.7;\omega) = -\frac{1}{0.7^4}\left(\frac{\Delta_v \overline{H}_{r\omega}}{\Delta_v Z_\omega}\right)^2 + \frac{1}{0.7^2}\frac{\Delta_v \overline{C}^*_{v\omega}}{\Delta_v Z_\omega}. \tag{18}$$

Figure 1(b) shows a plot of $f''(0.7;\omega)$ vs. ω. Symbols correspond to data obtained from RefProp 9.1 and equation (18). One can see that $f''(0.7;\omega)$ decreases with ω in a practically linear way. In figure 1(b) one can observe that the result for heavy water (filled square) clearly deviates from the observed trend for $f''(0.7;\omega)$. This behavior is related to a deviation in the RefProp 9.1 result of $\Delta_v \overline{C}^*_{v\omega}$ for heavy water (See Section 4 and figure 2(c)).

By taking as reference the acentric point, the CC vapor-pressure equation (8) becomes the well-known result [9,7,10]

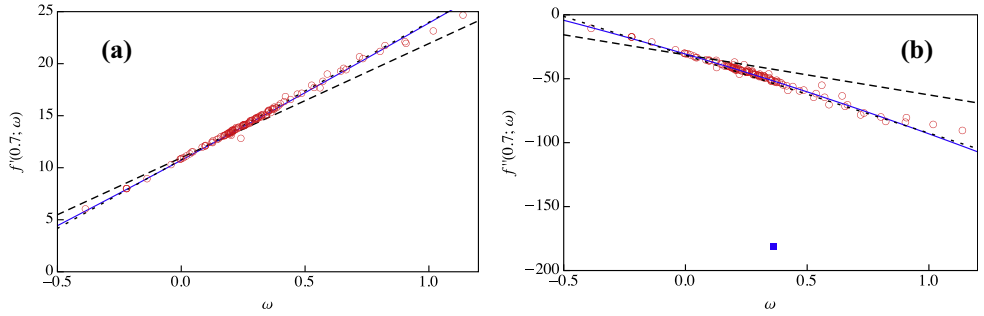

FIGURE 1. (a) The first temperature derivative of the natural logarithm of the vapor pressure at the acentric point $f'(0.7;\omega)$ vs. the acentric factor ω. The solid line represents the AW result given by equation (26), the dashed line represents the CC result (20), and the dotted line represents the LK result (23). (b) The second temperature derivative of the natural logarithm of the vapor pressure at the acentric point $f''(0.7;\omega)$ vs. the acentric factor ω. The solid line represents the AW result given by equation (27), the dashed line represents the CC result (21), and the dotted line represents the LK result (24). The symbols are the values obtained from RefProp 9.1 [8] (see text).

$$\ln p_r = f_{CC}(T_r;\omega) = \frac{7\ln 10}{3}(1+\omega)\left(1-\frac{1}{T_r}\right). \tag{19}$$

From this equation we obtain

$$f'_{CC}(0.7;\omega) = 10.9647(1+\omega) \tag{20}$$

and

$$f''_{CC}(0.7;\omega) = -31.3277(1+\omega). \tag{21}$$

Equations (20) and (21) are plotted by dashed lines in figure 1(a) and (b), respectively. One can see that the CC vapor pressure equation fails to reproduce the NIST results both for $f'(0.7;\omega)$ and for $f''(0.7;\omega)$, showing a similar linear behavior but with a different slope. Using equation (19), the average absolute relative deviation (AARD) for all fluids is 2.7% for $f'(0.7;\omega)$ and 15.6% for $f''(0.7;\omega)$. At this point it is interesting to note that using the values for the acentric factor ω listed in table 1 the CC vapor pressure equation (19) also fails to reproduce exactly (as one would expect from its definition) the RefProp 9.1 results for p_r at $T_r = 0.7$. The obtained absolute relative deviations are less than 0.602% for all fluids except for perfluoropentane (5.688%) and sulfur hexafluoride (1.966%). If these two fluids are not considered, the overall AARD for the vapor pressure at $T_r = 0.7$ is 0.0496%.

The second vapor-pressure equation that we check is the Lee–Kesler (LK) equation [11]

$$\ln p_r = f_{LK}(T_r;\omega) = \sum_{k=0}^{1}\left(A_k + \frac{B_k}{T_r} + C_k \ln T_r + D_k T_r^6\right)\omega^k, \tag{22}$$

where the eight coefficients A_k, B_k, C_k and D_k $(k = 0, 1)$ are given in table 2. In this case one has

$$f'_{LK}(0.7;\omega) = 10.7717 + 13.2089\,\omega \tag{23}$$

and

$$f''_{LK}(0.7;\omega) = -31.6983 - 60.8394\,\omega. \tag{24}$$

Equations (23) and (24) are plotted by dotted lines in figure 1(a) and (b), respectively. One can see that the LK vapor pressure equation gives rise to a good agreement with NIST data for both $f'(0.7;\omega)$ and $f''(0.7;\omega)$. Using equation (22), the AARD for all fluids is 1.2% for $f'(0.7;\omega)$ and 4.2% for $f''(0.7;\omega)$. The deviations for the vapor pressure at $T_r = 0.7$ are very similar to those obtained from the CC equation (19) with an overall AARD of 0.0503%, excluding perfluoropentane (5.694%) and sulfur hexafluoride (1.969%).

The third vapor-pressure equation we check is the Ambrose–Walton (AW) equation [12]

$$\ln p_r = f_{AW}(T_r;\omega) = \sum_{k=0}^{2}\left(\frac{A_k\tau + B_k\tau^{1.5} + C_k\tau^{2.5} + D_k\tau^5}{T_r}\right)\omega^k, \tag{25}$$

with $\tau = (1 - T_r)$ and where the twelve coefficients A_k, B_k, C_k and D_k $(k = 0, 1, 2)$ are given in table 3. From equation (25) we obtain

$$f'_{AW}(0.7;\omega) = 10.7187 + 12.7797\,\omega + 0.407899\,\omega^2 \tag{26}$$

and

$$f''_{AW}(0.7;\omega) = -30.6806 - 55.9725\,\omega - 6.45995\,\omega^2. \tag{27}$$

Equations (26) and (27) are plotted with solid lines in figure 1(a) and (b), respectively. One can see that the AW vapor pressure equation yields an excellent agreement with NIST data for both $f'(0.7;\omega)$ and $f''(0.7;\omega)$. Using equation (25), the AARD for all fluids is 0.7% for $f'(0.7;\omega)$ and 2.4% for $f''(0.7;\omega)$. Again, the deviations for the vapor pressure at the acentric point are the same than those obtained from the CC equation (19) with an overall AARD of 0.0496%, excluding perfluoropentane (5.688%) and sulfur hexafluoride (1.966%).

To conclude, in this section we have seen how the LK and the AW vapor pressure equations can also be used to determine with good agreement the first and second derivatives f' and f'' at the acentric point. Things are different for the CC equation that gives rise to noticeable deviations both for f' and f''.

3. The enthalpy of vaporization and the change in the compressibility factor at vaporization

Figure 2(a) shows a plot of the reduced enthalpy $\Delta_v\overline{H}_{r\omega}$ vs. ω. The symbols correspond to the NIST data obtained from RefProp 9.1 and listed in table 1. One can observe that $\Delta_v\overline{H}_{r\omega}$ increases as ω increases. Except for six oddball fluids (R40, methanol, methyl linolenate, methyl oleate, methyl palmitate, and methyl stearate), one can observe an excellent correlation between $\Delta_v\overline{H}_{r\omega}$ and the acentric factor ω. A quadratic fit excluding the six oddball fluids yields

$$\Delta_v\overline{H}_{r\omega} = 4.6027 + 6.6426\,\omega + 0.3836\,\omega^2, \tag{28}$$

with a coefficient of determination $R^2 = 0.9969$ and an overall AARD of 0.78%. The maximum absolute relative deviation (MARD) is obtained for perfluoropentane with a value of 3.98%.

Figure 2(b) shows a plot of the change of the compressibility factor as a function of the acentric factor. In this case one can observe that the $\Delta_v Z_\omega$ data do not follow a simple correlation with ω. However, taking into account the relation between $\Delta_v Z_\omega$, $\Delta_v\overline{H}_{r\omega}$, and $f'(0.7;\omega)$ given by equation (17) one can write

$$\Delta_v Z_\omega = \frac{\Delta_v\overline{H}_{r\omega}}{0.7^2 f'(0.7;\omega)} = \frac{9.3933 + 13.5563\,\omega + 0.7829\,\omega^2}{f'(0.7;\omega)}. \tag{29}$$

where we have used equation (28) and $f'(0.7;\omega)$ can be obtained from a given vapor-pressure equation. In particular, from equation (20) one obtains the CC result

TABLE 1
Critical temperature T_c, critical pressure p_c, acentric factor ω, reduced enthalpy of vaporization at the acentric point $\Delta_v\bar{H}_{r\omega}$ and its percent relative deviation (RD) from equation (28). The data have been obtained from RefProp 9.1 [8] for the 121 fluids considered in this work (see main text).

Fluid	T_c/K	p_c/kPa	ω	$\Delta_v\bar{H}_{r\omega}$	RD$\Delta_v\bar{H}_{r\omega}$
1-Butene	419.29	4005.1	0.192	5.8813	−0.186
Acetone	508.1	4700.	0.3071	6.4729	−3.182
Ammonia	405.4	11333.	0.256	6.18	−2.402
Argon	150.69	4863.0	−0.0022	4.623	0.755
Benzene	562.02	4907.28	0.211	6.0561	0.574
Butane	425.12	3796.	0.201	5.9533	−0.001
Undecane	638.8	1990.4	0.539	8.1896	−1.281
Dodecane	658.1	1817.0	0.574	8.5111	−0.362
Methylcyclohexane	572.2	3470.0	0.234	6.2204	0.68
Cis-butene	435.75	4225.5	0.202	5.9643	0.069
Propylcyclohhexane	630.8	2860.0	0.326	6.8111	0.031
Perfluorobutane	386.33	2323.4	0.371	7.1796	0.831
Perfluoropentane	420.56	2045.0	0.423	7.7916	3.984
Trifluoroiodomethane	396.44	3953.0	0.176	5.7806	−0.054
Carbon monoxide	132.86	3494.0	0.0497	5.0011	1.345
Carbon dioxide	304.13	7377.3	0.2239	6.1991	1.45
Carbonyl sulfide	378.77	6370.0	0.0978	5.2897	0.636
Cyclohexane	553.6	4080.5	0.2096	6.0742	1.026
Cyclopentane	511.72	4571.2	0.201	5.9399	−0.228
Cyclopropane	398.3	5579.7	0.1305	5.4975	0.389
Deuterium	38.34	1679.6	−0.136	3.6443	−1.706
Heavy water	643.85	21671.0	0.364	6.8974	−2.524
D4	586.49	1332.0	0.592	8.8763	2.328
D5	619.23	1161.46	0.658	9.177	0.407
D6	645.78	961.0	0.736	9.7195	0.206
Decane	617.7	2103.0	0.4884	7.9175	−0.265
DEE	466.7	3644.0	0.281	6.5098	0.157
DMC	557.0	4908.8	0.346	6.9326	−0.208
DME	400.38	5336.8	0.196	5.8905	−0.491
Ethylbenzene	617.12	3622.4	0.305	6.6378	−0.401
Ethane	305.32	4872.2	0.0995	5.2862	0.354
Ethanol	514.71	6268.0	0.646	8.9866	−0.749
Ethylene	282.35	5041.8	0.0866	5.2195	0.74
Fluorine	144.41	5172.4	0.0449	4.9691	1.355
Hydrogen sulfide	373.1	9000.0	0.1005	5.2973	0.436
Hydrogen chloride	324.55	8263.0	0.1288	5.2942	−3.22
Helium	5.2	227.61	−0.385	2.1209	0.882
Heptane	540.13	2736.0	0.349	6.9634	−0.063
Hexane	507.82	3034.0	0.299	6.6208	−0.035
Hydrogen	33.15	1296.4	−0.219	3.1405	−0.826
Isobutene	418.09	4009.8	0.193	5.8895	−0.162
Isohexane	497.7	3040.0	0.2797	6.4917	0.015
Isooctane	544.0	2572.0	0.303	6.6444	−0.095
Isopentane	460.35	3378.0	0.2274	6.1456	0.204
Isobutane	407.81	3629.0	0.184	5.8675	0.504
Krypton	209.48	5525.0	−0.0009	4.6118	0.325
MD2M	599.4	1227.0	0.668	9.1221	−0.976
MD3M	628.36	945.0	0.722	9.7477	1.529
MD4M	653.2	877.47	0.825	10.3231	−0.201
MDM	564.09	1415.0	0.529	8.3651	1.686
Methane	190.56	4599.2	0.0114	4.6925	0.298
Methanol	513.38	8215.85	0.5625	7.9221	−6.796
Methyl linoleate	799.0	1341.0	0.805	10.0589	−1.388
Methyl linolenate	772.0	1369.0	1.14	11.8573	−6.885
MM	518.7	1939.39	0.418	7.4833	0.494
Methyl oleate	782.0	1246.0	0.906	10.542	−3.735
Methyl palmitate	755.0	1350.0	0.91	10.4474	−4.955
Methyl stearate	775.0	1239.0	1.02	11.0876	−6.22
m-xylene	616.89	3534.6	0.326	6.7878	−0.312
Nitrous oxide	309.52	7245.0	0.162	5.7292	0.703
Neon	44.49	2678.6	−0.0387	4.3546	0.191
Neopentane	433.74	3196.0	0.1961	5.979	0.986
Nitrogen trifluoride	234.0	4460.7	0.126	5.4556	0.18
Nitrogen	126.19	3395.8	0.0372	4.8931	0.873
Nonane	594.55	2281.0	0.4433	7.6182	−0.06
Novec649	441.81	1869.0	0.471	7.8913	0.948
Octane	569.32	2497.0	0.395	7.2966	0.139
Orthohydrogen	33.22	1310.65	−0.218	3.1433	−0.94
Oxygen	154.58	5043.0	0.0222	4.7855	0.733
o-xylene	630.26	3737.5	0.312	6.6348	−1.173
Parahydrogen	32.94	1285.8	−0.219	3.1437	−0.722
Pentane	469.7	3370.0	0.251	6.3018	0.121
Propane	369.89	4251.2	0.1521	5.6446	0.402
Propylene	364.21	4555.0	0.146	5.6053	0.438
Propyne	402.38	5626.0	0.204	5.8167	−2.701
p-xylene	616.17	3531.5	0.324	6.7082	−1.297
R11	471.11	4407.64	0.1888	5.9053	0.589
R113	487.21	3392.2	0.2525	6.3619	0.902
R114	418.83	3257.0	0.2523	6.3793	1.195
R115	353.1	3129.0	0.248	6.3212	0.751
R116	293.03	3048.0	0.2566	6.3711	0.606
R12	385.12	4136.1	0.1795	5.8355	0.481
R1216	358.9	3149.53	0.333	6.8913	0.495
R123	456.83	3661.8	0.2819	6.5218	0.246
R1233zd	438.75	3572.6	0.305	6.6836	0.287
R1234yf	367.85	3382.2	0.276	6.4411	−0.375
R1234ze	382.51	3634.9	0.313	6.725	0.083
R124	395.42	3624.3	0.2881	6.5661	0.271
R125	339.17	3617.7	0.3052	6.6873	0.322
R13	302.0	3879.0	0.1723	5.7896	0.534
R134a	374.21	4059.28	0.3268	6.7825	−0.472
R14	227.51	3750.0	0.1785	5.8682	1.152
R141b	477.5	4212.0	0.2195	6.1257	0.758
R142b	410.26	4055.0	0.2321	6.1675	0.039
R143a	345.86	3761.0	0.2615	6.2776	−1.409
R152a	386.41	4516.75	0.2752	6.3691	−1.425
R161	375.25	5010.0	0.216	6.055	−0.007
R21	451.48	5181.2	0.2061	6.0164	0.471
R218	345.02	2640.0	0.3172	6.7659	0.259
R22	369.3	4990.0	0.2208	6.0886	0.008
R227ea	374.9	2925.0	0.357	7.054	0.44
R23	299.29	4832.0	0.263	6.2854	−1.445
R236ea	412.44	3420.0	0.369	7.1206	0.204
R236fa	398.07	3200.0	0.377	7.1584	−0.044
R245ca	447.57	3940.7	0.355	7.0434	0.486
R245fa	427.16	3651.0	0.3776	7.164	−0.024
R32	351.26	5782.0	0.2769	6.2957	−2.792
R365mfc	460.0	3266.0	0.377	7.1201	−0.581
R40	416.3	8263.0	0.243	5.572	−11.98
R41	317.28	5897.0	0.2004	5.7519	−3.431
RC318	388.38	2777.5	0.3553	7.1245	1.589
RE143a	377.92	3635.0	0.289	6.5002	−0.834
RE245cb2	406.81	2886.4	0.354	7.0026	0.005
RE245fa2	444.88	3433.0	0.387	7.227	−0.053
RE347mcc	437.7	2476.2	0.403	7.3759	0.46
Sulfur hexafluoride	318.72	3754.98	0.21	6.1069	1.511
Sulfur dioxide	430.64	7884.0	0.2557	6.3013	−0.396
Trans-butene	428.61	4027.3	0.21	5.9738	−0.683
Toluene	591.75	4126.3	0.2657	6.3612	−0.528
Water	647.1	22064.0	0.3443	6.7464	−2.799
Xenon	289.73	5842.0	0.0036	4.6519	0.542

TABLE 2
Coefficients for the Lee–Kesler vapor pressure equation (22) [11].

k	A_k	B_k	C_k	D_k
0	5.92714	−6.09648	−1.28862	0.169347
1	15.25180	−15.68750	−13.47210	0.435770

TABLE 3
Coefficients for the Ambrose–Walton vapor pressure equation (25) [12].

k	A_k	B_k	C_k	D_k
0	−5.97616	1.29874	−0.60394	−1.06841
1	−5.03365	1.11505	−5.41217	−7.46628
2	−0.64771	2.41539	−4.26979	3.25259

$$\Delta_v Z_\omega^{CC} = \frac{0.8567 + 1.2364\,\omega + 0.07140\,\omega^2}{1+\omega}, \tag{30}$$

using equation (23) yields

$$\Delta_v Z_\omega^{LK} = \frac{0.8720 + 1.2585\,\omega + 0.07268\,\omega^2}{1+1.2263\,\omega}, \tag{31}$$

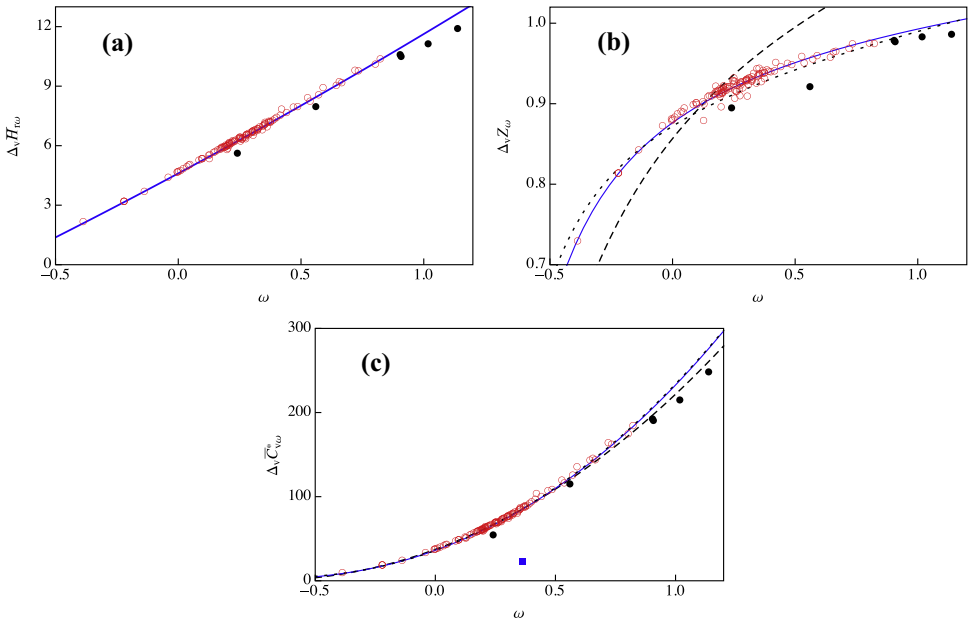

FIGURE 2. (a) The reduced enthalpy $\Delta_v\overline{H}_{r\omega}$ vs. the acentric factor ω. The solid line is the result of a quadratic fit to the data (symbols) (b) The change of the compressibility factor $\Delta_v Z_\omega$ vs. ω. The lines are results obtained from AW (solid), CC (dashed), and LK (dotted), and correspond to equations (32), (30), and (31), respectively. (c) The change in the constant-volume heat capacity $\Delta_v\overline{C}^*_{v\omega}$ vs. ω. The solid line represents the AW result (41), the dashed line represents the CC result (39), and the dotted line the LK result (40). In all cases the symbols are the values obtained from RefProp 9.1 [8] for the fluids listed in table 1. The oddball fluids are plotted with filled symbols (see text).

and inserting equation (26) into (29) gives rise to the AW result

$$\Delta_v Z_\omega^{AW} = \frac{0.8763 + 1.2647\,\omega + 0.07304\,\omega^2}{1 + 1.17406\,\omega + 1.24694\,\omega^2}. \quad (32)$$

Equations (30)–(32) are plotted in figure 2(b) with dashed, dotted and solid lines, respectively. One can see the excellent agreement between the results obtained from RefProp 9.1 and those obtained from the AW equation. In this case, using equation (32) and excluding the six oddball fluids, we obtain an overall AARD of 0.43% and a MARD of 2.69% for hydrogen chloride. Slightly inferior results are obtained from the LK equation (31), with an overall AARD of 0.96% and a MARD of 3.60% for helium. Finally, the CC equation (30) yields the worst agreement, with an overall AARD of 2.75% and a MARD of 12.64% for helium.

The most widely used expression for predicting the temperature dependence of the enthalpy of vaporization is the equation proposed by Watson [13,14]

$$\Delta_v\overline{H}_r(T_r) = B(1 - T_r)^{0.38}, \quad (33)$$

where the parameter B depends on the fluid and it can be obtained from a known point in the vapor-pressure curve. Choosing the acentric point as a reference, expression (33) becomes

$$\Delta_v\overline{H}_r(T_r;\omega) = \frac{\Delta_v\overline{H}_{r\omega}}{0.3^{0.38}}(1 - T_r)^{0.38}. \quad (34)$$

Taking into account equation (28), one obtains

$$\Delta_v\overline{H}_r(T_r;\omega) = (7.2729 + 10.4962\,\omega + 0.6061\,\omega^2)(1 - T_r)^{0.38}, \quad (35)$$

which provides the reduced enthalpy of vaporization in terms of the reduced temperature and the acentric factor. To authors knowledge this is the first time in the literature that the Watson equation for the enthalpy of vaporization is formulated in terms of the acentric factor. In general, equation (35) shows good agreement with RefProp 9.1 results, as shown in figure 3 for argon and propane. We note, however, that deviations are observed for water (see the solid lines in figure 3). These discrepancies can be ascribed in part to the difference ($\sim 2.8\%$) between the value of $\Delta_v\overline{H}_{r\omega}$ given by equation (28) and the RefProp 9.1 value reported in table 1 for water. If instead of equation (35) one considers equation (34) with the values of $\Delta_v\overline{H}_{r\omega}$ listed in table 1 a much better agreement is obtained for water (see the dashed lines in figure 3)

From equations (6) and (35) we obtain the relationship

$$\Delta_v Z(T_r;\omega) = \frac{\Delta_v\overline{H}_r(T_r;\omega)}{T_r^2 f'(T_r;\omega)} = \frac{(7.2729 + 10.4962\,\omega + 0.6061\,\omega^2)}{T_r^2 f'(T_r;\omega)}(1 - T_r)^{0.38}, \quad (36)$$

which allows one to calculate the change in the compressibility factor at vaporization from the slope function $f'(T_r;\omega)$.

Figure 4 compares RefProp 9.1 data for argon, propane and water with the results of equation (36) using three different prescriptions for $f(T_r;\omega)$ (AW, equation (25), CC (19), and LK (22)). The change in the compressibility factor at vaporization in argon is well described by the three prescriptions, with AW and LK yielding a slightly better agreement with RefProp 9.1 results than CC. In the cases of propane and water, CC clearly overestimates $\Delta_v Z(T_r;\omega)$ for low values of T_r while AW and LK still show a good agreement with RefProp 9.1 results.

4. The change in the constant-volume heat capacity at vaporization

An expression for the change in the constant-volume heat capacity at vaporization in terms of the derivatives f' and f'' can be readily obtained by substituting equation (6) into (7) and taking into account expression (10):

$$\Delta_v\overline{C}^*_v(T_r;\omega) = \left[\left(\frac{d\ln p_r}{dT_r}\right)^2 + \frac{d^2\ln p_r}{dT_r^2}\right]T_r^2\Delta_v Z(T_r;\omega) = \left[f'(T_r;\omega) + \frac{f''(T_r;\omega)}{f'(T_r;\omega)}\right]\Delta_v\overline{H}_r(T_r;\omega). \quad (37)$$

At the acentric point ($T_r = 0.7$) equation (37) becomes

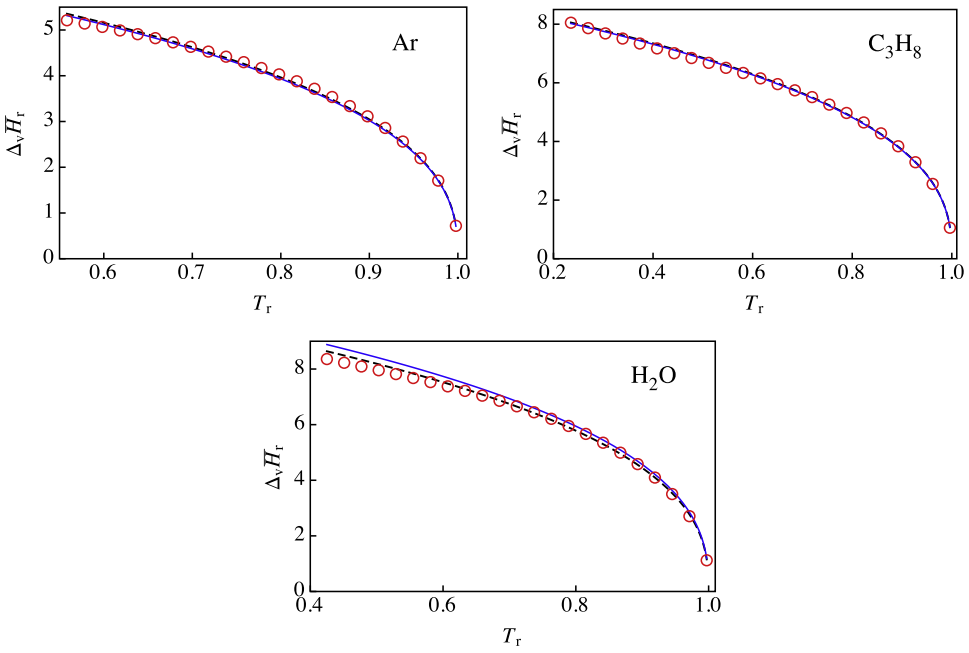

FIGURE 3. Enthalpy of vaporization $\Delta_v\overline{H}_r$ vs. the reduced temperature T_r for argon, propane and water. The symbols are RefProp 9.1 [8] results. The solid lines are obtained from equation (35). The dashed lines are obtained from equation (34) with the values of $\Delta_v\overline{H}_{r\omega}$ listed in table 1.

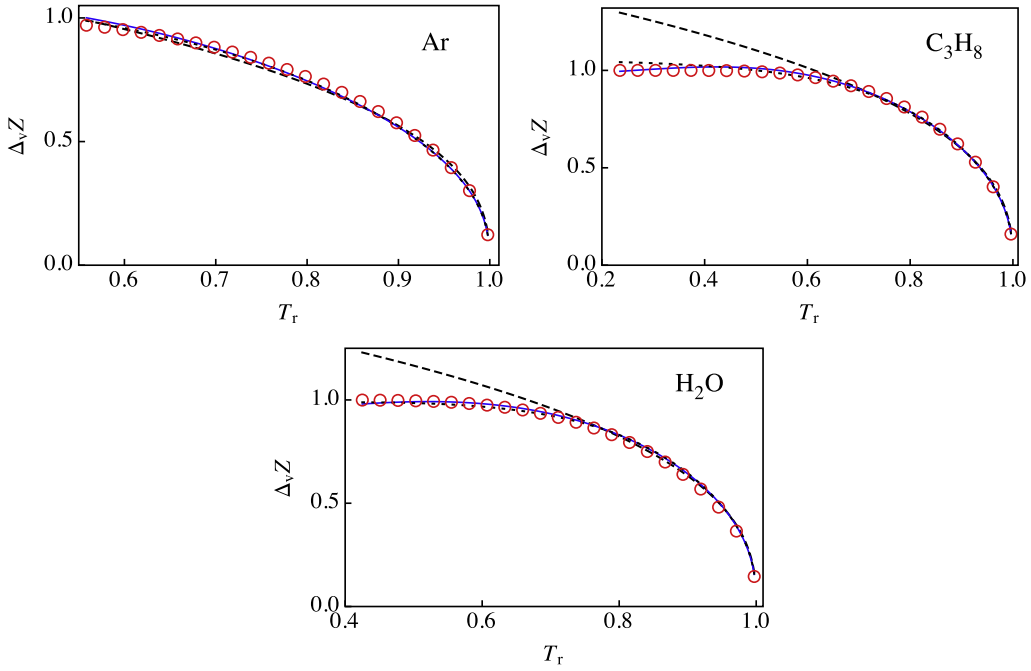

FIGURE 4. The compressibility factor at vaporization $\Delta_v Z$ vs. T_r for argon, propane and water. The symbols are RefProp 9.1 [8] results and the lines are obtained from equation (36) and equations (25) (AW, solid line), (19) (CC, dashed line), and (22) (LK, dotted line).

$$\Delta_v\overline{C}^*_{v\omega} = \left[f'(0.7;\omega) + \frac{f''(0.7;\omega)}{f'(0.7;\omega)}\right]\Delta_v\overline{H}_{r\omega}. \tag{38}$$

where $f'(0.7;\omega)$ and $f''(0.7;\omega)$ can be obtained from a given vapor-pressure equation and a suitable expression for $\Delta_v\overline{H}_{r\omega}$ is given by equation (28). For CC, using equations (20) and (21), equation (38) becomes

$$\Delta_v\overline{C}^{*CC}_{v\omega} = (8.1076 + 10.9647\omega)\Delta_v\overline{H}_{r\omega}. \tag{39}$$

For LK, from (23) and (24), equation (38) yields

$$\Delta_v\overline{C}^{*LK}_{v\omega} = \frac{7.8290 + 20.7698\omega + 16.1975\omega^2}{1 + 1.2263\omega}\Delta_v\overline{H}_{r\omega}. \tag{40}$$

Finally, for the AW case, substituting equations (26) and (27) into (38), one obtains

$$\Delta_v\overline{C}^{*AW}_{v\omega} = \frac{7.8564 + 20.3375\omega + 16.6555\omega^2 + 0.9727\omega^3 + 0.01552\omega^4}{1 + 1.1923\omega + 0.03805\omega^2}\Delta_v\overline{H}_{r\omega}. \tag{41}$$

Figure 2(c) shows a comparison between the above results (lines) for the dimensionless heat capacity $\Delta_v\overline{C}^*_{v\omega}$ in terms of the

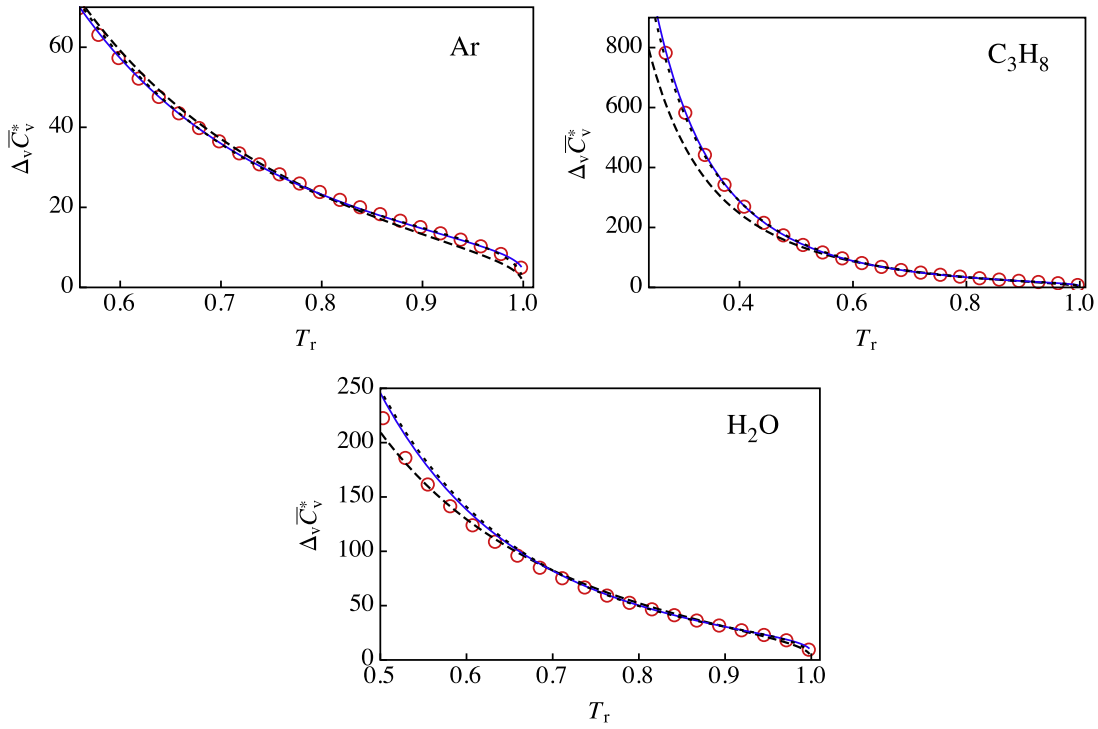

FIGURE 5. The change in the constant-volume heat capacity $\Delta_v\overline{C}^*_v(T_r;\omega)$ vs. T_r for argon, propane and water. The symbols are RefProp 9.1 [8] results and the lines are obtained from equation (37) and equations (25) (AW, solid line), (19) (CC, dashed line), and (22) (LK, dotted line).

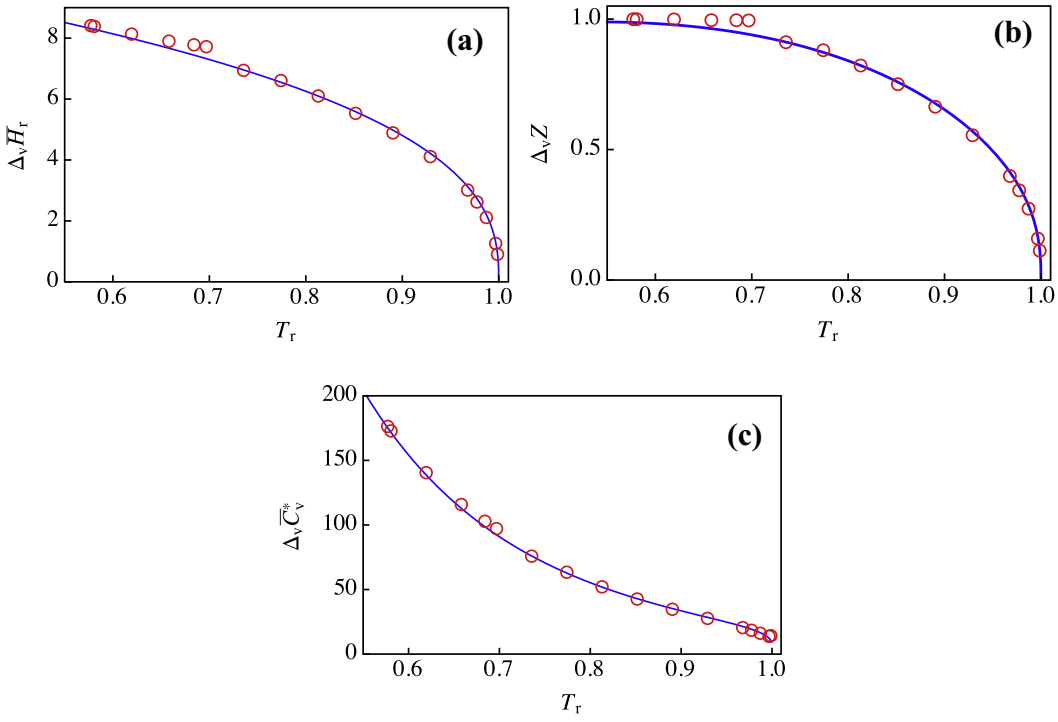

FIGURE 6. (a) Enthalpy of vaporization $\Delta_v\overline{H}_r$, (b) the compressibility factor at vaporization $\Delta_v Z$, and (c) the change in the constant-volume heat capacity $\Delta_v\overline{C}^*_v$ vs. T_r for perfluorobenzene. The symbols are experimental data [15]. The line in (a) is obtained from equation (35). The lines in (b) and (c) are AW results obtained from equation (25) and equations (36) (b) and (37) (c).

acentric factor and data (symbols) obtained from RefProp 9.1 [8]. One can observe that the monotonically increasing behavior of $\Delta_v\overline{C}^*_{v\omega}$ with ω is well described by equations (39)–(41) which are plotted in figure 2(c) with dashed, dotted, and solid lines, respectively. Apart from the six oddball fluids excluded from the fit (28) in figure 2(a), in figure 2(c) we plot with a filled square the RefProp 9.1 result for heavy water which shows a marked deviation from the general trend. In this case, using the AW equation (41) and excluding heavy water together with the above mentioned six oddball fluids, we obtain an overall AARD of 1.05%

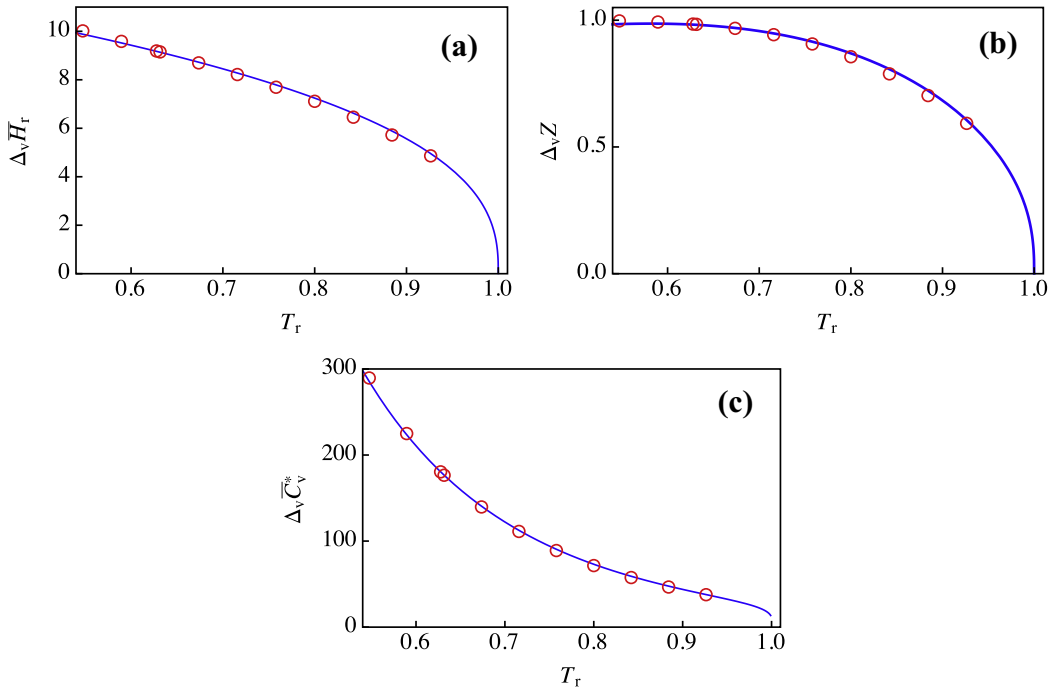

FIGURE 7. Same caption as in figure 6 but for perfluoro-n-heptane [16].

and a MARD of 6.81% for perfluoropentane. The LK equation (40) yields similar results with an overall AARD of 1.13% and a MARD of 6.24% for perfluoropentane. Finally, the CC equation (30) yields a slightly worse agreement, with an overall AARD of 1.91% and a MARD of 6.99% also for perfluoropentane. Like in previous situations, the large deviations observed for perfluoropentane are due to the lack of consistency between the RefProp 9.1 vapor pressure result for this fluid at $T_r = 0.7$ and the acentric factor listed in table 1.

Equation (37) with $\Delta_v \overline{H}_r(T_r;\omega)$ given by equation (35) and $f'(T_r;\omega)$ and $f''(T_r;\omega)$ obtained from the vapor pressure equations considered in this work are plotted with lines in figure 5 and compared with RefProp 9.1 results (symbols) for argon, propane and water. Overall, the AW and LK results for argon and propane show an excellent agreement with RefProp 9.1 data whereas the results for water show a noticeable deviation for low T_r. On the other hand, the CC results for argon and specially for propane compare less favorably with RefProp 9.1 data while the results for water show a much better agreement. In the later case, however, we believe that this agreement only reflect deviations that cancel each other out.

5. Comparison with experimental data

The LK and AW extended corresponding states expressions obtained in the preceding Sections have been shown to give very good agreement with RefProp 9.1 data. However, as previously commented, the RefProp 9.1 data are not experimental results and therefore it seems interesting to compare the predictions of the new expressions with experimental data for fluids different from those included in the RefProp 9.1 computer program. The goal of this Section is to perform this comparison in order to test the performance of the new corresponding states results. Restricted by the availability of the required experimental data, two fluids have been considered, namely, perfluorobenzene and perfluoro-n-heptane.

Figure 6 shows the comparison between experimental data [15] and theoretical predictions for perfluorobenzene. Figure 6(a) compares the results of equation (35) with experimental data for the enthalpy of vaporization with excellent agreement for $T_r > 0.7$. The differences for $T_r \leqslant 0.7$ are due to the use of an ideal gas model for obtaining the low temperature gas phase results in the experimental data [15]. Figure 6(b) and (c) compare experimental data with AW results obtained from equation (25) and equations (36) and (37), respectively. Like in figure 6(a) we obtain excellent agreement except for $T_r \leqslant 0.7$. The only data used as an input in the theoretical predictions are the critical temperature $T_c = 516.66$ K, the critical pressure $p_c = 3273.2$ kPa, and the acentric factor $\omega = 0.3965$ [15].

Figure 7 compares experimental data for perfluoro-n-heptane [16] with the theoretical predictions of this work. In all cases we obtain excellent agreement in the whole range of temperatures considered. In this case we considered $T_c = 475$ K, $p_c = 1650$ kPa, and $\omega = 0.5611$ [16].

6. Summary

In this work we have analyzed the behavior of the first and second derivatives of the natural logarithm of the reduced saturation pressure with respect to the reduced temperature at the acentric point. Using data for the 121 fluids considered in the RefProp 9.1 program [8] we have obtained a well defined behavior for these derivatives with excellent agreement with the results of the AW and LK vapor pressure equations. Since the first derivative is related to the ratio between the enthalpy of vaporization and the change in the compressibility factor at vaporization, we have also studied these two quantities at the acentric point. We have obtained that the enthalpy of vaporization at the acentric point presents an excellent correlation with the acentric factor. Combining this correlation with the first derivative of different vapor pressure equations we have obtained that both AW and LK yield excellent agreement with RefProp 9.1 data for the change in the

compressibility factor at vaporization whereas the CC equation gives rise to important discrepancies.

Considering the acentric point as a reference in the Watson equation, we have derived a new equation (35) for the temperature dependence of the enthalpy of vaporization in terms of the acentric factor. The results of this equation show excellent agreement with RefProp 9.1 data for different fluids. From equation (35) and the relation between $\Delta_v\overline{H}_r(T_r;\omega)$, $\Delta_v Z(T_r;\omega)$, and $f'(T_r;\omega)$, we have also obtained an expression for the temperature dependence of the change in the compressibility factor at vaporization in terms of ω, with good agreement with RefProp 9.1 data for different fluids in the case of the AW and LK equations, with noticeable deviations for the CC equation at low temperatures.

In equation (37) we have expressed the change in the constant-volume heat capacity at vaporization in terms of the derivatives f' and f'', and the enthalpy of vaporization. This equation turns out to give excellent agreement with RefProp 9.1 data at the acentric point for all of the considered fluids except for heavy water where important deviations are observed (see figure 2(c)). Using the AW and the LK vapor pressure equations in equation (37) yields excellent agreement with RefProp 9.1 results for the temperature dependence of the constant-volume heat capacity at vaporization of argon and propane with some deviations for water at low temperatures.

Finally, in order to compare with experimental results we have considered two fluids (perfluorobenzene and perfluoro-n-heptane) for which the required data are available. In both cases the agreement with the new results is excellent.

Acknowledgements

We thank financial support by Ministerio de Economía y Competitividad of Spain under Grant ENE2013-40644-R.

References

[1] C.N. Yang, C.P. Yang, Phys. Rev. Lett. 13 (1964) 303–305.
[2] E.A. Guggenheim, J. Chem. Phys. 13 (1945) 253–261.
[3] E.A. Guggenheim, Thermodynamics, North-Holland, Amsterdam, 1967.
[4] K.S. Pitzer, J. Am. Chem. Soc. 77 (1955) 3427–3433.
[5] K.S. Pitzer, D.Z. Lippmann, R.F. Curl, C.M. Huggins, D.E. Petersen, J. Am. Chem. Soc. 77 (1955) 3433–3440.
[6] B.E. Poling, J.M. Prausnitz, J.P. O'Connell, The Properties of Gases and Liquids, McGraw-Hill, New York, 2001. fifth edition.
[7] S. Velasco, J.A. White, J. Chem. Eng. Data 56 (2011) 1163–1166.
[8] E.W. Lemmon, M.L. Huber, M.O. McLinden, NIST Standard Reference Database 23: Reference fluid thermodynamic and transport properties-REFPROP, version 9.1, National Institute of Standards and Technology, Standard Reference Data Program, Gaithersburg, 2013.
[9] M.C. Edmister, Pet. Refin. 37 (1958) 173–179.
[10] S. Velasco, J. White, J. Chem. Thermodyn. 68 (2014) 193–198.
[11] B.I. Lee, M.G. Kesler, AIChE J. 21 (1975) 510–527.
[12] D. Ambrose, J. Walton, Pure Appl. Chem. 61 (1989) 1395–1403.
[13] K. Watson, Ind. Eng. Chem. 23 (1931) 360–364.
[14] F.L. Román, J.A. White, S. Velasco, A. Mulero, J. Chem. Phys. 123 (2005) 124512–124516.
[15] S.V. Stankus, R.A. Khairulin, Int. J. Thermophys. 27 (2006) 1110–1122.
[16] W.V. Steele, R.D. Chirico, S.E. Knipmeyer, A. Nguyen, J. Chem. Eng. Data 42 (1997) 1021–1036.

JCT 14-547